Structural vulnerability of quantum networks

Ang-Kun Wu,[1,2,3] Liang Tian,[4] Bruno Coelho Coutinho,[5] Yasser Omar,[5,6] and Yang-Yu Liu[1,7,*]

[1]*Channing Division of Network Medicine, Brigham and Women's Hospital, Harvard Medical School, Boston, Massachusetts 02115, USA*
[2]*Department of Physics, Zhejiang University, Hangzhou, Zhejiang 310027, China*
[3]*Department of Physics and Astronomy, Rutgers University, Piscataway, New Jersey 08854, USA*
[4]*Department of Physics and Institute of Computational and Theoretical Studies, Hong Kong Baptist University, Kowloon, Hong Kong, China*
[5]*Instituto de Telecomunicações, Physics of Information and Quantum Technologies Group, Lisbon, Portugal*
[6]*Instituto Superior Técnico, Universidade de Lisboa, Lisbon, Portugal*
[7]*Center for Cancer Systems Biology, Dana-Farber Cancer Institute, Boston, Massachusetts 02115, USA*

(Received 23 September 2019; accepted 1 April 2020; published 7 May 2020)

Structural vulnerability of a network can be studied via two key notions in graph theory: articulation points (APs) and bridges, representing nodes and edges whose removal will disconnect the network, respectively. Fundamental properties of APs and bridges in classical random networks have been studied recently. Yet, it is unknown if those properties still hold in quantum networks. Quantum networks allow for the transmission of quantum information between physically separated quantum systems. They play a very important role in quantum computing, quantum communication, and quantum sensing. Here we offer an analytical framework to study the structural vulnerability of quantum networks in terms of APs and bridges. In particular, we analytically calculate the fraction of APs and bridges for quantum networks with arbitrary degree distribution and entangled qubits in pure states. We find that quantum networks with swap operations have lower fractions of APs and bridges than their classical counterparts. Moreover, we find that quantum networks under low-degree swap operations are substantially more robust against AP attacks than their classical counterparts. These results help us better understand the structural vulnerability of quantum networks and shed light on the design of more robust quantum networks.

DOI: 10.1103/PhysRevA.101.052315

I. INTRODUCTION

Mathematically, a network can be represented by a graph $\mathcal{G}(\mathcal{V}, \mathcal{E})$, where $\mathcal{V} = \{1, \ldots, N\}$ is the node set and $\mathcal{E} \subset \mathcal{V} \times \mathcal{V}$ is the edge set. The degree k of a node is the number of its nearest neighbors. There are two key notions in graph theory that naturally describe the structural vulnerability of a network: articulation points (APs) and bridges. Here, APs [1–3] (or bridges [4]) are nodes (or edges) in a graph whose removal will disconnect the graph and hence increase the number of connected components. By definition, APs and bridges ensure the connectivity of a network and represent potential targets of attack if one aims for immediate damage to a network. For instance, shutting down APs or bridges in air traffic networks or power grids may causes major disorder to the infrastructure networks [5,6]. Malfunction of APs or bridges in wireless sensor networks will block data transmission between different components [7]. Lethal mutations have a higher frequency in the group of proteins that are highly connected APs than do proteins that participate in genetic interactions, or viable mutations [8]. Thus, through studying APs and bridges, we can obtain more insights for the structure vulnerability of real-world networks.

Recently, fundamental properties of APs and bridges in classical complex networks have been systematically studied [9,10]. It was found that real-world networks tend to have less APs than their degree-preserving randomizations but they have similar bridge fractions as their degree-preserving randomizations. (Here degree-preserving randomization means that we keep the degree of each node unchanged, but completely rewire the links connecting them.) Analytical approaches for AP and bridge statistics have been proposed for complex networks with arbitrary degree distributions. It was found that with increasing mean degree c, the fraction of APs (denoted as f_{AP}) increases first until it reaches its maximum value at a particular mean degree c_{AP}, and then gradually decreases to zero in the large c limit. For the fraction of bridges (denoted as f_{b}), it will stay at one until the emergence of the giant connected component (GCC) at the percolation threshold c^*. After that, f_{b} will decrease monotonically to zero in the large c limit.

More interestingly, when we remove all the existing APs from a network, known as the greedy AP removal (GAPR) process, we may generate some new APs. If we repeat GAPR until there is no AP left, the final network will end up being either completely empty or a residual giant bicomponent (RGB), in which any two nodes are connected by at least two independent paths and hence no AP exists. In other words, such an infinite-step GAPR leads to a RGB percolation transition. Surprisingly, the RGB percolation transition is *hybrid*, i.e., the relative size of the RGB has a jump at the percolation threshold as a first-order phase transition but also has a critical singularity as a second-order phase transition.

*Corresponding author: yyl@channing.harvard.edu

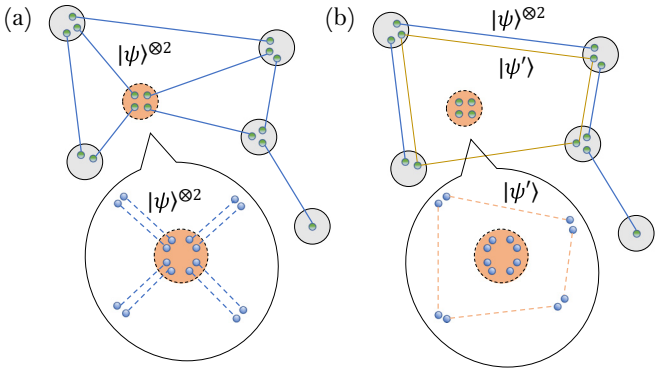

FIG. 1. Demonstration of a small quantum network and the 4-swap operation. (a) In this quantum network, edges (blue lines) represent entangled qubits (small green circles). Qubits are located in different spatial stations (gray circles), which represent nodes in the quantum network. The orange circle is a node of degree 4 that is going to be swapped. Inset: each edge (solid blue lines) contains two partially entangled pairs (dashed blue lines); blue circles are individual qubits contained in green circles; dashed lines of the same color are the same partially entangled states ($|\psi\rangle$). (b) The network after 4-swap operation. The yellow lines (dashed or solid) are new entangled pairs $|\psi'\rangle$ with the same SCP as $|\psi\rangle$, generated by the swap operation (Bell measurement on the central orange node).

By contrast, any finite steps of GAPR will lead to a normal percolation transition, which belongs to the same universality class of the classical GCC percolation transition. Therefore, this GAPR process results in a very rich phase diagram with two fundamentally different types of percolation transitions.

The study of APs and bridges in classical networks does provide us quite different perspectives on the organizational principles of complex networks. It can help us prevent the failure of real network functions, design more resilient systems, or find more effective destruction strategies for malicious networks.

With all these intriguing results on APs and bridges for classical networks, an interesting question arises naturally: if we are dealing with networks in quantum information, will there be nontrivial behavior for APs and bridges? To address this question, we need to define what kind of quantum networks to work with. This paper is hence organized as follows. In Sec. II, we specify the setting of ideal quantum complex networks and introduce the quantum swap operation. In Sec. III, we demonstrate how the quantum swap operation works in such quantum networks and how it affects the AP and bridge structure in the network. In Sec. IV, we provide an analytical framework of AP and bridge calculation in such quantum complex networks and compare the analytical results with numerical simulations. In Sec. V, we perform numerical simulations of the GAPR process to show the RGB percolation transition. The final section is devoted to conclusion and discussion.

II. QUANTUM COMPLEX NETWORKS AND SWAP OPERATION

In general, an ideal quantum network is connected by entangled states, as shown in Fig. 1(a), where nodes are stations (shown in gray) in physical locations with a set of particles (qubits, shown in green) entangled with other particles in other stations with pure states. For theoretical simplicity, we focus on full-fledged ideal quantum networks with no dephasing. Although quantum dephasing is one of the major concerns when building a quantum network today, it was been proposed that in the future the effects of quantum dephasing could be minimized by using an error correction and a fully fault and loss tolerant code [11–13]. While full-fledged quantum networks are still under development, the studies about robust protocols and measures of building quantum networks from small scale have been proposed [14,15]. Here, we explore the theoretical properties of large-scale quantum networks. These entangled pairs of particles serve as connection links such that quantum operations like Bell measurements [16,17] and entanglement swapping [18–20] can be applied. Here, qubits resembling bits in classic computer science are quantum objects with two eigenstates $|0\rangle$ and $|1\rangle$ in Dirac's notation, with which infinite quantum states can be formed due to the superposition principle [16,18,19]. An edge (shown in blue) between two nodes means an entangled state connecting two qubits in separated locations [18,19]. We can simply use integers i and j to denote two stations or nodes.

In such a network we consider that entangled qubits are and stay in a pure state form; hence the edge between two nodes can be expressed by the joint wave function:

$$\begin{aligned}|\psi_{ij}\rangle &= \sqrt{1-p_s/2}|0\rangle_i \otimes |0\rangle_j + \sqrt{p_s/2}|1\rangle_i \otimes |1\rangle_j \\ &= \sqrt{1-p_s/2}|00\rangle + \sqrt{p_s/2}|11\rangle, \end{aligned} \tag{1}$$

which, due to entanglement, cannot be decomposed as a direct product of two states, i.e., $|\phi\rangle_i \otimes |\phi\rangle_j$ [16,17]. Here, p_s is the singlet conversion probability (SCP), quantifying the probability of converting this partially entangled state into the maximally entangled state (singlet) $|\psi_{ij}\rangle = \sqrt{1/2}(|00\rangle + |11\rangle)$ using local operations and classical communication (LOCC) [21,22]. For perfect quantum communication, only maximally entangled states (which, via quantum teleportation, are perfect single-use quantum channels [19]) can be used. To this end, we only consider end-to-end maximally entangled states as finally existing connections.

The key difference between quantum and classical networks is that we can apply quantum operations to change the topology of networks. In the model proposed by Perseguers *et al.* [18], where each connection is one entangled pair, if two nodes are in the same connected component, they can be connected by a singlet pure state, which is reduced to the percolation theory in classical networks. In order to implement entanglement swapping, from Cirac and Cuquet *et al.* [19,23], network structure is initially formed with prescribed degree distribution and each connection (initial edge) is formed by two identical partially entangled states, with the same SCP [Fig. 1(a), inset]. The probability of the existence of an edge changes since one of the two states surviving in the conversion is sufficient [without distillation [19], namely the new conversion probability becomes $p_2 = 1 - (1 - p_s)^2$]. The purpose of such a design is to realize the local operation—q-swap, which converts a node with initial q degree (q-star structure) into a q-circle before the conversion, connecting all the neighbors successively in a circle while separating

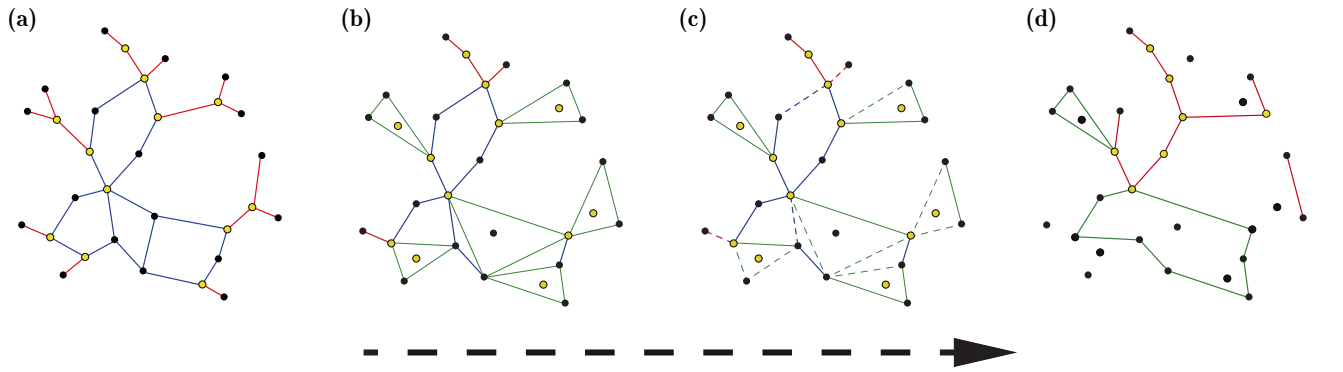

FIG. 2. Topology changes of a quantum network under 3-swap operation. (a) Initial network generated by ER random graph. Here black and yellow nodes are normal nodes and APs, respectively. Blue and red edges are normal edges and bridges, respectively. (b) Network of (a) after 3-swap. Green edges are entangled states emerging after 3-swap. (c) Network of (b) when singlet conversion $p_s = 0.5$ is applied to finalize edges (maximally entangled states). Connections in dash lines are entangled states deleted by singlet conversion. (d) Final topology of the network with less APs and bridges after singlet conversion.

the center [Fig. 1(b)] [19]. The strategy is realized by Bell measurement and can ensure the connections between the neighbors have the same SCP. In principal, one can define an initial connection formed by any number of entangled pairs. Two is the minimum to realize the q-swap strategy and change the topology of the network, which maximize the quantum operation effect. Note that no swap operation can be performed for a node if any of its neighbors has been swapped, because the swapped states are no longer the same quantum states as the original ones (Fig. 1, blue and yellow lines). In this way, Cuquet *et al.* has shown that the entanglement percolation threshold of quantum complex networks can be substantially decreased compared to the classical model as well as regular lattices [23]. In this process, the order of swap does matter, but the effect of order is negligible for system size larger than 100 under random selection (see Appendix A) because the probability of nodes with the same degree forming large cluster is very rare.

III. APs, BRIDGES, AND SWAP OPERATION

Despite quantum complex networks having merit in establishing long-distance entanglement between arbitrary nodes through entanglement percolation [19], we have no idea how they react to the breakdown of nodes or edges. Naturally, we wonder how the fundamental properties of APs and bridges in classical networks [9,10] will change in the quantum regime, particularly under quantum swap operation.

In Fig. 2, we demonstrate how the topology of original random-network-based quantum networks changes under quantum swap and singlet conversion. We can clearly see the numbers of bridges and APs decrease and the size of GCC evolve during the process. Though a series of nodes are isolated due to swap operation, the connectivity within the remaining part is enhanced. Since swapping nodes here are selected randomly, in case we hope to keep particular stations or connections, we can avoid swapping such nodes or edges by using other q-swaps or swapping only nearby q-nodes.

IV. ANALYTICAL FRAMEWORK

We now show our statistical results for large Erdős-Rényi (ER) random graphs using both numerical simulations and analytic calculations. (Results for scale-free networks can be found in Appendix B.) Both APs and bridges in a graph can be identified via a linear-time algorithm based on depth-first search [24].

To develop the analytical framework, we adopt the local tree approximation (LTA), which assumes the absence of finite loops in the thermodynamic limit (i.e., as the network size $N \to \infty$) and allows only infinite loops [9,25–28]. Though small loops can be formed under quantum swaps, the LTA still stands since these loops are local.

Generating functions $G_0(x) = \sum_{k=0}^{\infty} P(k)x^k$ and $G_1(x) = \sum_{k=1}^{\infty} P_1(k)x^{k-1}$ are very useful in calculating key quantities of random graphs, such as the mean component size and the size of GCC [27,29]. Here, $P(k)$ is the degree distribution and $P_1(k) = kP(k)/c$ is the excess degree distribution, where $c = \sum_{k=0}^{\infty} kP(k)$ is the mean degree. To analytically compute the fractions of APs and bridges, we introduce the generating function $\tilde{H}_1(x)$ for the size distribution of the components that are reachable by choosing a random initial edge (before swap and conversion) and following one of its ends. The notation $\tilde{H}_0(x)$ is reserved for the generating function of the size distribution of the components that a randomly chosen node locates in. Note that here we consider the other end of the edge is not swapped; then every node of degree q can be swapped. Considering the swap operation and SCP, we can write down the self-consistent equation for $\tilde{H}_1(x)$ with single swap [19]:

$$\tilde{H}_1(x) = 1 - p_2 + p_2 x G_1[\tilde{H}_1(x)] + \tilde{H}_{1,q}(x), \tag{2}$$

where $p_2 = 2p - p^2$ is the SCP for two entangled states without distillation; $\tilde{H}_{1,q}(x)$ is the term modified for q-swap operation,

$$\tilde{H}_{1,q}(x) = P_1(q)\{(p_2 - 1) - p_2 x[\tilde{H}_1(x)]^{q-1} + C_q(x)\}, \tag{3}$$

with $C_q(x) = \sum_{l=0}^{q-2}(l+1)p^l(1-p)^2\{xG_1[\tilde{H}_1(x)]\}^l + [qp^{q-1}(1-p) + p^q]\{xG_1[\tilde{H}_1(x)]\}^{q-1}$.

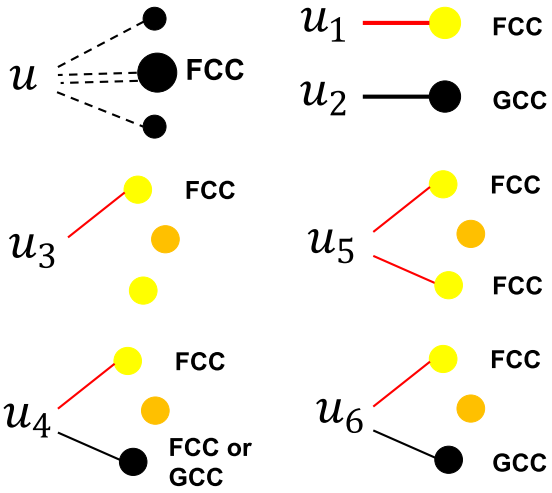

FIG. 3. New structural elements need to be considered in analyzing APs and bridges. Different dashed lines are different partial entangled states. Each dashed line is of the same SCP. Solid lines are edges after conversion. Red lines represent bridges. Points represent nodes, where yellow ones are APs and orange ones are isolated. Black lines and points are edges and nodes of uncertain state.

For a given p, we define $u := \tilde{H}_1(1)$, representing the probability that following a randomly chosen initial edge to one of its end nodes the node belongs to a finite connected component (FCC) after removing this edge (including size of zero, where the final edge doesn't even exist: $p_3 = (1 - p_2)[1 - P_1(q)] + P_1(q)(1 - p)^2$) (see Fig. 3).

Under the LTA, the essence of identifying bridges and APs is that at least one of their neighbors is in an FCC, a counterpart of the GCC, when discarding the connecting edges. Otherwise, nodes or edges will be in an infinite loop and cannot separate components. In other words, a bridge must have one end connecting to an FCC so that removing it will segregate the FCC; an AP should have at least one edge along with the other end belonging to an FCC, except for those whose degree is one.

In order to analyze bridges and APs in quantum networks, we need to be equipped with more detailed structures concerning FCC and GCC. Since a node cannot be swapped if its neighbors have been swapped, we need to consider the probability η that a randomly chosen q-degree node will be swapped in a q-swap operation. Actually, for multiple q-swap, each η_q can be computed through self-consistent equations and single q-swap has approximate expression $\eta \approx [1 + qP_1(q)/2]^{-1}$ [19,30]. In our framework, we use the simulated swap probability. Besides, through simple conversion, the probability of a randomly chosen edge along with an q-degree end being swapped is actually also η. Based on the above analysis, we can write down the following crucial structural elements (see Fig. 3).

(i) $u_1 := G_1(u) - \eta P_1(q) u^{q-1}$ is the probability that a randomly chosen final edge is unswapped and along with an end belonging to FCC.

(ii) $u_2 := 1 - \eta P_1(q) - u_1$ is the probability that a randomly chosen final edge is unswapped and along with an end belonging to GCC.

(iii) $u_3 = (1 - p)^2 \sum_{l=1}^{q-2} [pG_1(u)]^l + (1 - p)[pG_1(u)]^{q-1}$ is the probability that a randomly chosen initial edge is swapped and has only one new final edge belonging to FCC.

(iv) $u_4 = (1 - p)^2 \sum_{l=2}^{q-2} p^l \sum_{k=1}^{l-1} G_1(u)^k + (1 - p)p^{q-1} \sum_{k=1}^{q-2} G_1(u)^k$ is the probability that a randomly chosen initial edge is swapped and has two new final edges and ends, one of which belongs to FCC.

(v) $u_5 = (1 - p)^2 \sum_{l=2}^{q-2} (l - 1)[pG_1(u)]^l + (q - 2)(1 - p)p^{q-1} G_1(u)^{q-1}$ is the probability that a randomly chosen initial edge is swapped and along with has two new final edges and ends, both belonging to FCC.

(vi) $u_6 = u_4 - u_5$ is the probability that a randomly chosen initial edge is swapped and has two new final edges and ends, one belonging to FCC and the other belonging to GCC.

Following what we did for classical networks [9,10], now we can write down the analytical expressions for the size of bridges and APs normalized by total edges (before conversion) and total nodes. In particular, the probability of a randomly chosen node to be an AP is given by

$$\begin{aligned} f_{\mathrm{AP}} = 1 &- G_0[1 - u + p_3 - 2P_1(q)u_6] \\ &- cG_1(p_3)[u - p_3 - P_1(q)u_5] \\ &- \eta P(q)\{1 - [1 - u + p_3 - 2P_1(q)u_6]^q \\ &- qP_1(q)p_3^{q-1}[u - p_3 - P_1(q)u_5]\}, \end{aligned} \tag{4}$$

where the second term excludes nodes with all edges and neighbors in GCC and the third term excludes nodes that become leaves (degree equals to one) and the lengthy fourth term deletes all q-degree nodes isolated by q-swap.

For the probability of a randomly chosen initial edge being a bridge, there are two cases. In the first case, the initial edge will not be swapped (with a probability $[1 - \eta P_1(q)]^2$). The probability of being a bridge is then given by

$$p_{\mathrm{b}} = \left(2u_1u_2 + u_1^2\right)p_2, \tag{5}$$

which means at least one side of the edge finally belongs to FCC.

In the second case, the initial edge will be swapped (with a probability $2\eta P_1(q) - [\eta P_1(q)]^2$). Then there can either be one or two bridges emerging with probabilities denoted by p_{b1} and p_{b2}, respectively. We have

$$\begin{aligned} p_{\mathrm{b1}} = &2\eta P_1(q)\{2u_2u_6 + 2u_3[1 - \eta P_1(q)] \\ &+ 2u_1[p(1 - p) - u_3]\}, \end{aligned} \tag{6}$$

where $2\eta P_1(q)$ is the probability of one side (node) being swapped and the three terms in the curly braces represent three one-bridge scenarios. And

$$p_{\mathrm{b2}} = 2\eta P_1(q)\{2u_1u_6 + u_5[1 - \eta P_1(q)]\}, \tag{7}$$

where the two terms in the curly braces are two two-bridge scenarios. Note that each bridge is also shared by the other end who is not in the initial consideration. Therefore, we need to divide the probability by 2 and the final bridge fraction (i.e., normalized by the total initial number of edges) is given by

$$f_{\mathrm{b}} = p_{\mathrm{b}} + (p_{\mathrm{b1}} + p_{\mathrm{b2}})/2. \tag{8}$$

Note that, for $q = 2$, the process is equivalent to deleting all two-degree nodes and connecting their neighbors directly.

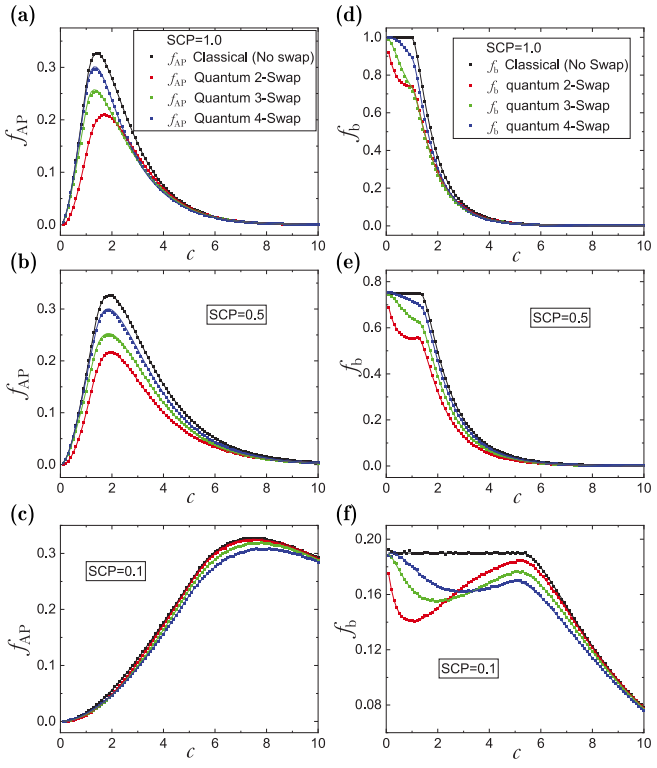

FIG. 4. Articulation points and bridges in quantum networks generated from canonical random graphs. Points are simulation results in ER random graphs, which initially have one million nodes. SCP $= p_s$ is the singlet conversion probability that a single entangled state will be converted to the maximally entangled state. c is the mean degree of initial quantum networks. (a)–(c) Fraction of APs as a function of initial mean degree c and $p_s = 1.0, 0.5, 0.1$. (d)–(f) Fraction of bridges (normalized by initial total edges) as a function of initial mean degree c and $p_s = 1.0, 0.5, 0.1$.

There is no loop and therefore the expression of f_b is slightly different:

$$f_b = p_b + \eta P_1(q)(u_1 + u_2 u_1) p_2. \tag{9}$$

In Fig. 4, we show the fractions of APs and bridges as functions of mean degree c in initial ER random graphs with Poisson degree distribution $P(k) = e^{-c}c^k/k!$ [31]. Across different values of SCP, the fractions of APs and bridges under swap operations are all smaller compared to the no-swap case. The effect of different q-swaps upon APs and bridges varies at different values of SCP and mean degree c. At low c, small q swap, for instance 2-swap, is more prominent than high q swap as 4-swap; at high c the situation is reversed, which generates the crossover behavior of different swaps. This is intuitive due to the degree distributions at different mean degrees. At low c, small-degree nodes populate more, which makes small q swap more effective and vice versa.

Furthermore, SCP, which controls the survival rate of entangled states and final mean degree of networks, also changes the effect of swaps both in the position (initial mean degree c) and curve shape [see Fig. 4(h)]. For SCP $= 1.0$, the q-swap operation isolates most of q-degree nodes and decreases the total number of existing edges (for instance, 2-swap operation works as a contraction for 2-degree nodes). Furthermore, q-swap creates local loops and alternative paths for some pairs of nodes and thus decreases APs and bridges [Fig. 2(e)]. For SCP < 1.0, which effectively decreases the final mean degree, for a given q-swap, decreasing SCP will cause both curves $f_{AP}(c)$ and $f_b(c)$ to shift right. A comparison between quantum networks and a null model after we consider the node isolation and edge deletion due to q-swap and singlet conversion is provided in Appendix C.

V. RESIDUAL GIANT BICOMPONENT (RGB)

To further study the vulnerability of networks after swap, we study the RGB percolation transition associated with the infinite-step GAPR (i.e., we iteratively remove APs from a network until there is no AP left) [9]. Figure 5 shows that the RGB percolation threshold becomes lower when applying different swap strategies with SCP $= 1.0$ and SCP $= 0.5$ quantum networks, which means the robustness of networks concerning AP attack is greatly improved in this circumstance. At SCP $= 1.0$, this q-swap operation can also be thought of as a sacrifice of q-degree nodes for stronger connection between the rest.

However, when SCP < 1.0, not all swap strategies work better than the null model (i.e., no swap). In the case SCP $=$ 0.5, 6-swap even have higher critical mean degree than null model (see Appendix D). This is because swapped high-degree nodes are harder to complete a connected local loop with their neighbors when SCP < 1.0 (p_s^n decreases as n increases). And the swap operation separates neighbors of the central node. The distance between neighbors of the swapped node are only two edges away from each other, but in a loop, the largest distance can be half of the degree. Thus the connections between the remaining nodes get weakened by high degree swap for SCP < 1.0. In the end, it delays the percolation of the GAPR process.

We also show the phase diagram of GAPR under scale-free (SF) networks in Fig. 6, which shows the RGB percolation shift of 3-swapped quantum networks at a given initial mean degree $c = 6$. This phase diagram demonstrates that the change of RGB percolation transition is even more pronounced than the GCC percolation for scale-free networks. For instance, the first red circle from the left in Fig. 6 indicates that the swap operation induces an RGB, while the no-swap case does not.

VI. CONCLUSION

In conclusion, we studied the structural vulnerability of ideal quantum networks with pure entangled states under single q-swap operation. In particular, we calculated the fractions of APs and bridges in quantum networks with arbitrary degree distributions. We presented both simulation and analytical results, which agree well with each other. Interestingly, we found that single q-swap operation reduces the fractions of APs and bridges in quantum networks and therefore enhances the robustness of quantum networks under attack. When applying the GAPR process to quantum networks, we find that small-degree swap decreases the RGB percolation threshold, namely decreasing the vulnerability of networks under greedy

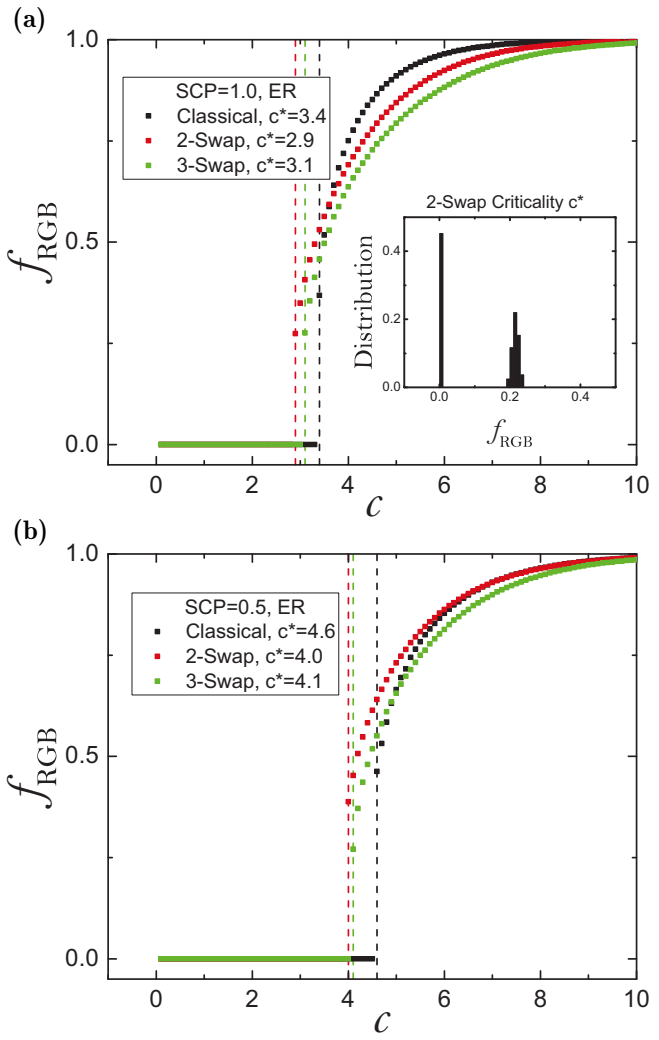

FIG. 5. Residual giant bicomponent (RGB) fraction as a function of initial mean degree c in different networks. Dots are simulations in random graphs with one million nodes in different SCP $p_s = 1.0, 0.5$. Different colors represent various swap strategies. Vertical lines mark transition points. There is no RGB percolation at SCP $= 0.1$. (a) Fraction of RGB as a function of initial mean degree c under SCP 1.0. The inset shows the distribution of RGB fraction at the transition point $c* = 3.1$ over 1000 realizations. The two-peak distribution shows that this is the first order phase transition as the nonswap case [9]. (b) Fraction of RGB as a function of initial mean degree c under SCP 0.5.

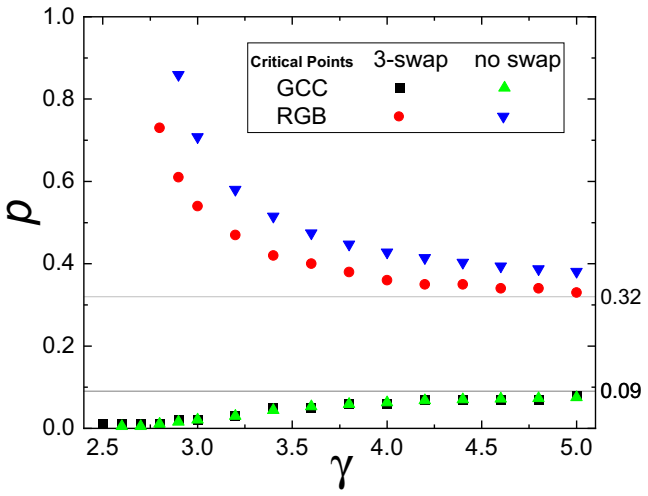

FIG. 6. Phase diagram associated with the GAPR process for scale-free (SF) networks at $c = 6$ with or without 3-swap. Colored symbols are critical points (p_c) at different γ for SF networks. The two horizontal gray lines are critical results for ER networks ($\gamma \to \infty$ limit) under 3-swap. Here, GCC means percolation transition without AP removal. The results without swap are obtained from theoretical calculation [19], while 3-swap results are from simulations.

AP removal. The presented results may shed light on the design of more robust quantum networks.

ACKNOWLEDGMENTS

Y.Y.-L. is supported by grants from the John Templeton Foundation (Award No. 51977) and National Institutes of Health (R01AI141529, R01HD093761, UH3OD023268, U19AI095219, and U01HL089856). B.C. and Y.O. acknowledge the support from Fundação para a Ciência e a Tecnologia (Portugal), namely through project UIDB/EEA/50008/2020, as well as from projects TheBlinQC and QuantHEP supported by the EU H2020 QuantERA ERA-NET Cofund in Quantum Technologies and by Fundação para a Ciência e a Tecnologia (FCT) (QuantERA/0001/2017 and QuantERA/0001/2019, respectively), from the John Templeton Foundation (JTF) project NQuN (ID No. 60478), and from the EU H2020 Quantum Flagship project QMiCS (No. 820505).

Y.-Y.L. conceived and designed the project. A.-K.W. performed all the analytical and numerical calculations. A.-K.W.

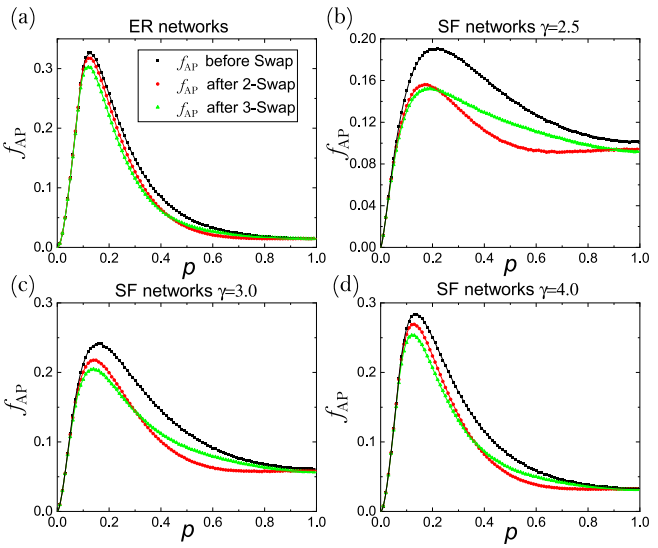

FIG. 7. APs in different quantum networks generated from canonical random graphs. Points are simulation results in random graphs, which initially have one million nodes and mean degree $c = 6.0$, and curves are analytical results. (a) ER random graph. (b) Scale-free networks with $\gamma = 2.5$. (c) Scale-free networks with $\gamma = 3.0$. (d) Scale-free networks with $\gamma = 4.0$.

TABLE I. Statistical error of random swap operation.

System size (mean degree 6, 6-swap, run 20 times, error=sd)	Swap probability no. of nodes swapped/ no. of nodes in the degree)	Size of GCC after swap	f_{AP} after swap (divide by total edges before swap	f_b after swap (divide by total edges before swap)	Existing edges
100	0.57(5)	0.68(1)	0.020(1)	0.006 7(1)	0.976(5)
1000	0.64(2)	0.888(3)	0.020 4(7)	0.006 8(2)	0.997 4(4)
10 000	0.695(3)	0.889 2(5)	0.014 2(2)	0.004 73(5)	0.999 90(3)

and Y.-Y.L. wrote the manuscript. Other authors edited the manuscript.

APPENDIX A: EFFECT OF RANDOMNESS OF SWAP OPERATION

The effect of randomness of swap operation is shown in Table I. We test different system sizes and each for 20 realizations. From Table I we can see that even with small system size and small realizations the error of randomness is very small. The detailed theoretical discussion of swap probability can be found in [30].

APPENDIX B: SCALE-FREE RESULTS

In Fig. 7(a) and Fig. 8(a), we show the fractions of bridges and APs as functions of conversion probability p in initial ER random graphs with Poisson degree distribution $P(k) = e^{-c}c^k/k!$ [31]. We find that our analytical results agree well with our simulations. Both the numbers of bridges and APs decrease compared to classical cases (black lines and symbols). This is because, for one thing, q-swap operation isolates most of the q-degree nodes and makes the total number of existing edges less (for instance, 2-swap operation) and, for another, q-swap creates many local loops and makes an alternative path for some pairs of nodes and thus decreases bridges and APs. However, since the newly created entangled states from swap have smaller SCP, they could also create some more bridges (see Fig. 2), which accounts for the crossover between curves of 2-swap and 3-swap.

We also calculate f_b and f_{AP} for scale-free (SF) networks with power-law degree distribution $P(k) \sim k^{-\lambda}$ generated by the static model [32–34]. For SF networks, the smaller the

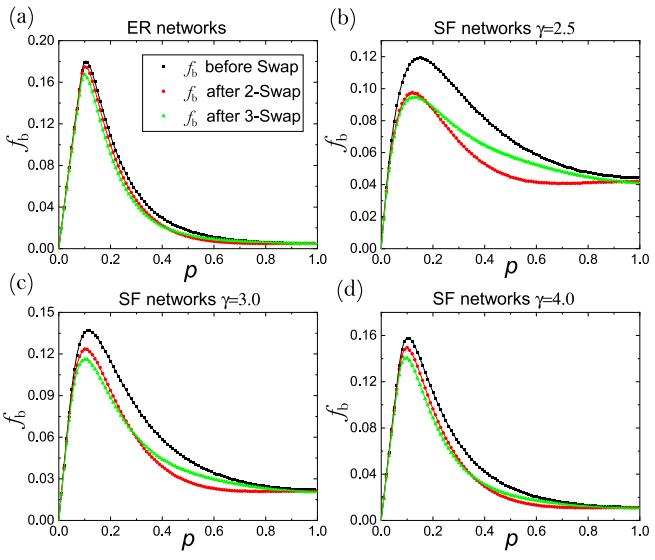

FIG. 8. Bridges in different quantum networks generated from canonical random graphs. Points are simulation results in random graphs, which initially have one million nodes and mean degree $c = 6.0$, and curves are analytical results. p is the probability that a single entangled state will be converted to the maximally entangled state. Bridges are normalized by initial total edges when $c = 6.0$. (a) ER random graph. (b) Scale-free networks with $\gamma = 4.0$. (c) Scale-free networks with $\gamma = 3.0$. (d) Scale-free networks with $\gamma = 2.5$.

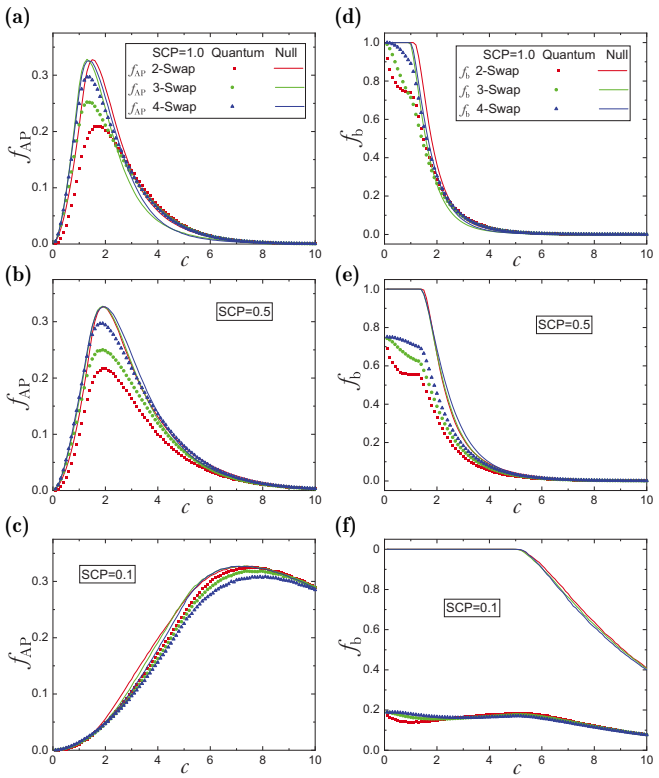

FIG. 9. Comparison with null model after q-swap and singlet conversion. Points are simulation results as a function of the mean degree c in initial ER random graphs of size $N = 10^6$. The solid curves are results of ER random graphs with mean degrees c after q-swap and singlet conversion. (a)–(c) Fraction of APs and $p_s = 1.0, 0.5, 0.1$. (d)–(f) Fraction of bridges and $p_s = 1.0, 0.5, 0.1$.

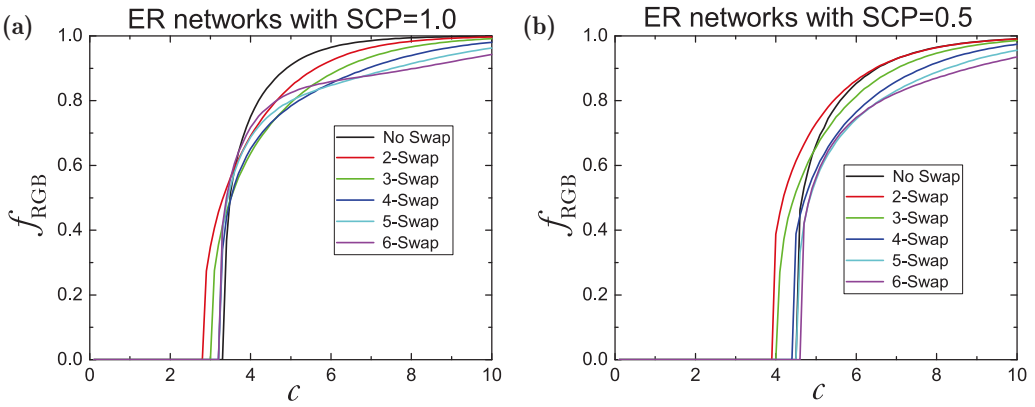

FIG. 10. RGB percolation transitions in different networks. Curves are simulation results in random graphs, which have one million nodes in two different SCP 1.0 and 0.5. Different colors represent various swap strategies. (a) Fraction of RGB as a function of initial mean degree c under SCP 1.0. (b) Fraction of RGB as a function of initial mean degree c under SCP 0.5.

degree exponent λ, the larger comparative decrease of vulnerable structure [see Figs. 7 and 8(b)–8(d)].

APPENDIX C: NULL MODEL AFTER NODE ISOLATION AND SINGLET CONVERSION

In these quantum complex networks, quantum operations (e.g., q-swap and singlet conversion) lead to node isolation and edge deletion. If we take these into consideration, a slightly different null model can be defined as random networks with the mean degree to be that of final quantum network. The finite size effect is negligible in the thermodynamics limit. In Fig. 9, we compare the fractions of APs and bridges in ER networks (solid curves, mean degrees of which are set to be the mean degrees after we apply the swap, remove isolated nodes, and singlet conversion) and the results calculated from our analytical framework.

For SCP $= 1.0$ (maximal entangled states) or before singlet conversion [see Figs. 9(a) and 9(d)], the fractions of APs and bridges show greater decrease than the null model used in the main text at low mean degree. For high mean degree, the fractions of APs and bridges in this new null model are much lower than those calculated through our analytical framework. This can be interpreted as follows. At low mean degree, 2,3,4-swaps isolate 2,3,4-degree nodes, which further decreases the mean degree of the whole network. By contrast, at high mean degree, the isolation of 2,3,4-degree nodes increases the mean degree of the whole network by removing low-degree nodes. The effect of this null model is basically a nonuniform shift of our no-swap case.

If we consider partially entangled states, SCP < 1, this new null model generally has larger fractions of APs and bridges than what we calculated from our analytical framework [see Figs. 9(b), 9(c) 9(e), and 9(f)]. The larger AP fraction is because, in this new null model, the AP fraction is computed over the nodes excluding isolated ones (swapped ones). When SCP < 1, we decrease the mean degree of the final network, which is equivalent to focusing on the low mean-degree part of Fig. 9(a). The reason that the fraction of bridges always starts from 1 instead of scaling with SCP is due to the definition of the bridge fraction. In this new null model, the bridge fraction is defined over the final existing edges. However, in the main text, the bridge fraction is defined over the original mean degree (the label of x axis).

APPENDIX D: GAPR WITH HIGH SWAP

Figure 10 shows the GAPR percolation with higher q-swap operation. In the case of SCP $= 0.5$, 6-swap even has a higher critical mean degree than the null model (no swap). This is because swapped high-degree nodes are harder to complete a connected local loop with their neighbors when SCP $<$ 1.0 (p_s^n decreases as n increases). And the swap operation separates between neighbors of the central node. The distance between neighbors of the swapped node are only two edges away from each other, but in a loop, the largest distance can be half of the degree. Thus the connections between the remaining nodes get weakened by high degree swap for SCP < 1.0. In the end, it delays the percolation of the GAPR process.

[1] M. Behzad and G. Chartrand, *Introduction to the Theory of Graphs* (Allyn and Bacon, Boston, 1972).
[2] F. Harary *et al.*, *Graph Theory* (Addison-Wesley, Reading, MA, 1969).
[3] P. Holme, B. J. Kim, C. N. Yoon, and S. K. Han, Attack vulnerability of complex networks, Phys. Rev. E **65**, 056109 (2002).
[4] B. Bollobás, *Modern Graph Theory, Volume 184 of Graduate Texts in Mathematics* (Springer-Verlag, New York, 1998).
[5] E. Conti, S. Cao, and A. Thomas, Disruptions in the US airport network, arXiv:1301.2223.
[6] W. T. Cox and T. Considine, Architecturally significant interfaces for the smart grid, in *Proceedings of Grid-Interop: The Road to an Interoperable Grid, Denver, Colorado, USA* (GridWise® Architecture Council (GWAC), Richland, WA, 2009).
[7] Y. F. Hassan and F. M. Gebreel, Articulation points detection in wireless sensor networks, Int. J. Intelligent Inf. Process **3**, 87 (2012).

[8] N. Pržulj, D. A. Wigle, and I. Jurisica, Functional topology in a network of protein interactions, Bioinformatics **20**, 340 (2004).
[9] L. Tian, A. Bashan, D.-N. Shi, and Y.-Y. Liu, Articulation points in complex networks, Nat. Commun. **8**, 14223 (2017).
[10] A.-K. Wu, L. Tian, and Y.-Y. Liu, Bridges in complex networks, Phys. Rev. E **97**, 012307 (2018).
[11] W. J. Munro, K. Azuma, K. Tamaki, and K. Nemoto, Inside quantum repeaters, IEEE J. Sel. Top. Quantum Electron. **21**, 78 (2015).
[12] S. Muralidharan, J. Kim, N. Lütkenhaus, M. D. Lukin, and L. Jiang, Ultrafast and Fault-Tolerant Quantum Communication across Long Distances, Phys. Rev. Lett. **112**, 250501 (2014).
[13] W. J. Munro, A. M. Stephens, S. J. Devitt, K. A. Harrison, and K. Nemoto, Quantum communication without the necessity of quantum memories, Nat. Photon. **6**, 777 (2012).
[14] S. Das, S. Khatri, and J. P. Dowling, Robust quantum network architectures and topologies for entanglement distribution, Phys. Rev. A **97**, 012335 (2018).
[15] S. Khatri, C. T. Matyas, A. U. Siddiqui, and J. P. Dowling, Practical figures of merit and thresholds for entanglement distribution in quantum networks, Phys. Rev. Research **1**, 023032 (2019).
[16] M. A. Nielsen and I. L. Chuang, *Quantum Computation and Quantum Information* (Cambridge University Press, Cambridge, UK, 2010).
[17] N. Chandra and R. Ghosh, Quantum entanglement in electron optics, *Quantum Entanglement in Electron Optics: Generation, Characterization, and Applications*, Springer Series on Atomic, Optical, and Plasma Physics Vol. 67 (Springer-Verlag, Berlin, 2013), p. 1.
[18] S. Perseguers, M. Lewenstein, A. Acín, and J. I. Cirac, Quantum random networks, Nat. Phys. **6**, 539 (2010).
[19] M. Cuquet and J. Calsamiglia, Entanglement Percolation in Quantum Complex Networks, Phys. Rev. Lett. **103**, 240503 (2009).
[20] B. Coecke, The logic of entanglement, in *Horizons of the Mind. A Tribute to Prakash Panangaden* (Springer, New York, 2014), pp. 250–267.
[21] R. F. Werner, Quantum states with Einstein-Podolsky-Rosen correlations admitting a hidden-variable model, Phys. Rev. A **40**, 4277 (1989).
[22] G. Vidal, Entanglement of Pure States for a Single Copy, Phys. Rev. Lett. **83**, 1046 (1999).
[23] A. Acín, J. I. Cirac, and M. Lewenstein, Entanglement percolation in quantum networks, Nat. Phys. **3**, 256 (2007).
[24] R. Tarjan, Depth-first search and linear graph algorithms, SIAM J. Comput. **1**, 146 (1972).
[25] M. Molloy and B. Reed, A critical point for random graphs with a given degree sequence, Random Struct. Alg. **6**, 161 (1995).
[26] D. S. Callaway, M. E. J. Newman, S. H. Strogatz, and D. J. Watts, Network Robustness and Fragility: Percolation on Random Graphs, Phys. Rev. Lett. **85**, 5468 (2000).
[27] M. E. J. Newman, S. H. Strogatz, and D. J. Watts, Random graphs with arbitrary degree distributions and their applications, Phys. Rev. E **64**, 026118 (2001).
[28] S. N. Dorogovtsev, A. V. Goltsev, and J. F. F. Mendes, Critical phenomena in complex networks, Rev. Mod. Phys. **80**, 1275 (2008).
[29] M. Newman, *Networks* (Oxford University Press, Oxford, 2018).
[30] M. Cuquet and J. Calsamiglia, Limited-path-length entanglement percolation in quantum complex networks, Phys. Rev. A **83**, 032319 (2011).
[31] P. Erdös and A. Rényi, On the evolution of random graphs, Publ. Math. Inst. Hung. Acad. Sci. **5**, 17 (1960).
[32] K.-I. Goh, B. Kahng, and D. Kim, Universal Behavior of Load Distribution in Scale-Free Networks, Phys. Rev. Lett. **87**, 278701 (2001).
[33] M. Catanzaro and R. Pastor-Satorras, Analytic solution of a static scale-free network model, Eur. Phys. J. B **44**, 241 (2005).
[34] J.-S. Lee, K.-I. Goh, B. Kahng, and D. Kim, Intrinsic degree-correlations in the static model of scale-free networks, Eur. Phys. J. B **49**, 231 (2006).